

Direct Reprogramming of Human Fibroblasts to Functional and Expandable Hepatocytes

Pengyu Huang,^{1,10} Ludi Zhang,^{1,10} Yimeng Gao,^{1,10} Zhiying He,^{2,10} Dan Yao,³ Zhitao Wu,³ Jin Cen,¹ Xiaotao Chen,¹ Changcheng Liu,² Yiping Hu,² Dongmei Lai,⁴ Zhenlei Hu,⁵ Li Chen,⁶ Ying Zhang,⁶ Xin Cheng,¹ Xiaojun Ma,⁶ Guoyu Pan,³ Xin Wang,^{7,8,9} and Lijian Hui^{1,*}

¹State Key Laboratory of Cell Biology, Institute of Biochemistry and Cell Biology, Shanghai Institutes for Biological Sciences, Chinese Academy of Sciences, Shanghai 200031, China

²Department of Cell Biology, Second Military Medical University, Shanghai 200433, China

³Center for Drug Safety Evaluation and Research, Shanghai Institute of Materia Medica, Chinese Academy of Sciences, Shanghai 201203, China

⁴The International Peace Maternity and Child Health Hospital, School of Medicine, Shanghai Jiaotong University, Shanghai 200030, China

⁵Renji Hospital, School of Medicine, Shanghai Jiaotong University, Shanghai 200127, China

⁶Laboratory of Biomedical Material Engineering, Dalian Institute of Chemical Physics, Chinese Academy of Sciences, Dalian 116023, China

⁷Key Laboratory of National Education Ministry for Mammalian Reproductive Biology and Biotechnology, Inner Mongolia University, Hohhot 010021, China

⁸Department of Laboratory Medicine and Pathology, Stem Cell Institute, University of Minnesota, Minneapolis, MN 55455, USA

⁹Hepatoscience Incorporation, 4062 Fabian Way, Palo Alto, CA 94303, USA

¹⁰These authors contributed equally to this work

*Correspondence: ljhui@sibcb.ac.cn

<http://dx.doi.org/10.1016/j.stem.2014.01.003>

SUMMARY

The generation of large numbers of functional human hepatocytes for cell-based approaches to liver disease is an important and unmet goal. Direct reprogramming of fibroblasts to hepatic lineages could offer a solution to this problem but so far has only been achieved with mouse cells. Here, we generated human induced hepatocytes (hiHeps) from fibroblasts by lentiviral expression of FOXA3, HNF1A, and HNF4A. hiHeps express hepatic gene programs, can be expanded in vitro, and display functions characteristic of mature hepatocytes, including cytochrome P450 enzyme activity and biliary drug clearance. Upon transplantation into mice with concanavalin-A-induced acute liver failure and fatal metabolic liver disease due to fumarylacetoacetate dehydrolase (Fah) deficiency, hiHeps restore the liver function and prolong survival. Collectively, our results demonstrate successful lineage conversion of nonhepatic human cells into mature hepatocytes with potential for biomedical and pharmaceutical applications.

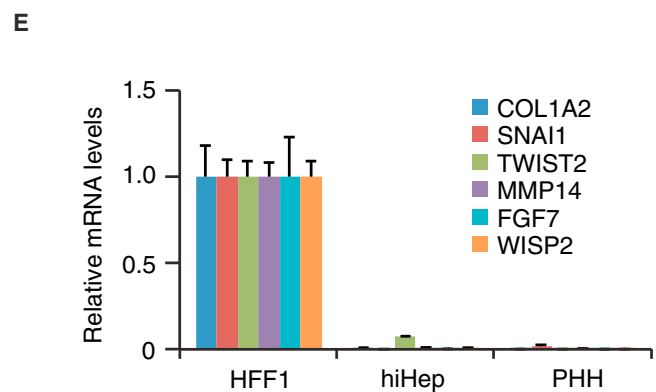
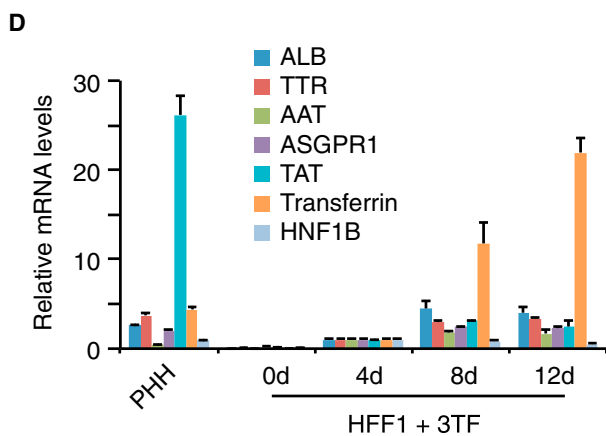
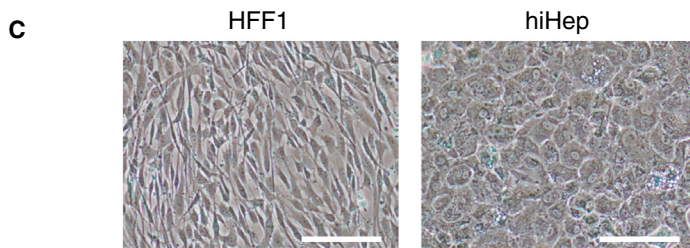
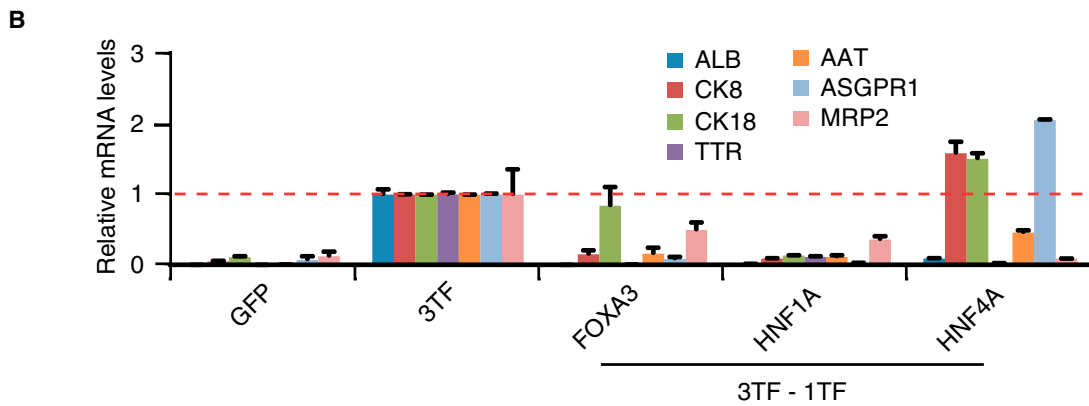
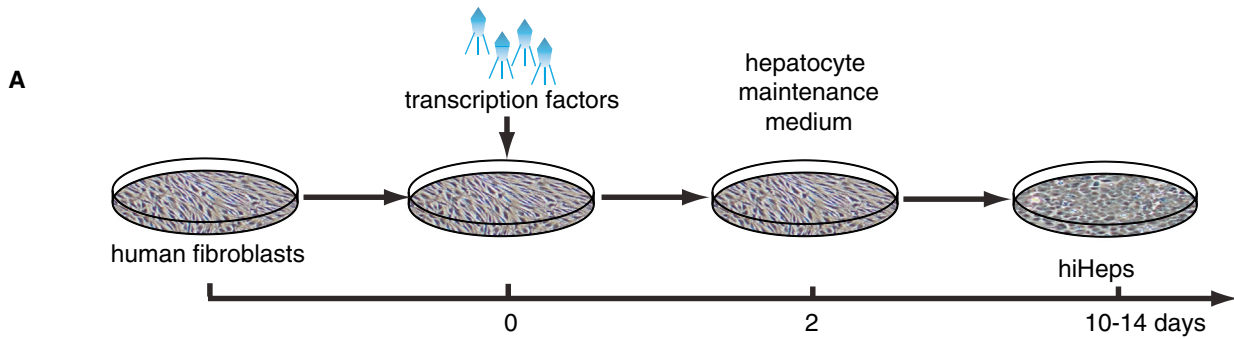
INTRODUCTION

Overexpression of lineage-specific transcription factors has been broadly used to change cell fates (Vierbuchen and Wernig, 2011; Yamanaka and Blau, 2010). Direct cell lineage conversion through reprogramming facilitates the generation of donor organ-independent cells for applications in regenerative medicine or personalized disease modeling (Cherry and Daley, 2012; Tiscornia et al., 2011; Vierbuchen and Wernig, 2011). Whereas

several studies have successfully converted mouse fibroblasts into other cell types, it is well accepted that human cells are resistant to lineage reprogramming (Nam et al., 2013; Pang et al., 2011; Qiang et al., 2011). Transdifferentiation into neuronal cells (iN) has been demonstrated in human cells; however, the in vivo functions of human iN, especially their application in therapeutic treatment, have not yet been thoroughly characterized (Pang et al., 2011; Qiang et al., 2011). A recent study managed to reprogram human fibroblasts into cells with a cardiac fate, but these cells lacked mature cardiac functions (Nam et al., 2013). Furthermore, transdifferentiated cells are proliferation arrested, which precludes them from expanding in large numbers for in vivo measurements and biomedical applications (Graf and Enver, 2009).

The liver is a pivotal organ in regulating many physiological processes, such as glycogen storage, lipid metabolism, plasma protein secretion, and xenobiotic detoxification (Hengstler et al., 2005). Liver diseases, such as liver metabolic diseases and fulminant liver failure, are important causes of death worldwide. Liver transplantation is currently the only curative treatment for these diseases at the end stages. Primary human hepatocyte (PHH) transplantation has been recently evaluated in clinics as an alternative to organ transplantation (Dhawan et al., 2010). On the other hand, liver support devices containing functional hepatocytes have been developed in order to allow the liver to recover from acute liver failure (Carpentier et al., 2009). Besides the therapeutic applications, hepatocytes are widely used for disease modeling, such as hepatitis C virus infection and humanized animal models, and for drug metabolism and pharmacokinetics analysis, e.g., hepatobiliary disposition of drug candidates (Azuma et al., 2007; Gómez-Lechón et al., 2004; Lázaro et al., 2007). However, the demand for liver organs and functional hepatocytes far exceeds the supply of cadaveric livers and liver tissues from living donors. Generation of surrogate hepatocytes is the key to meeting these demands.

We and others have previously demonstrated that mouse fibroblasts could be directly converted to hepatic lineage by



(legend on next page)

defined transcription factors (Huang et al., 2011; Sekiya and Suzuki, 2011). The extension of these findings to human cells is a challenge that must be overcome for biomedical and pharmaceutical applications (Cherry and Daley, 2012; Tiscornia et al., 2011; Vierbuchen and Wernig, 2011). Here, we report the efficient generation of human-induced hepatocytes (hiHeps) from human fetal fibroblasts (HFFs), adult fibroblasts (HAFs), and adult adipose tissue-derived mesenchymal stem cells (AD-MSCs) by *FOXA3*, *HNF1A*, and *HNF4A*, which differ from factors used for mouse cells. hiHeps show mature hepatic functions, specifically, cytochrome P450 (CYP) enzyme activities and biliary excretion of drug compounds. Notably, we demonstrate the therapeutic effects of hiHeps on fumarylacetoacetate hydroxylase (Fah)-deficiency-induced metabolic liver disease and concanavalin A (Con A)-induced acute liver failure. These results indicate that hiHeps could be applied in cellular therapies, disease modeling, and drug discovery.

RESULTS

Generation of hiHeps by Direct Lineage Conversion

Mouse fibroblasts have been converted into induced hepatocytes (iHeps) (Huang et al., 2011; Sekiya and Suzuki, 2011). In this study, we wished to induce functionally mature human iHeps (hiHeps). We first generated primary human fetal limb fibroblasts (HFF1) and demonstrated that HFF1 cells were free of fetal hepatoblasts (Figures S1A and S1B available online). Based on findings in mouse cells (Huang et al., 2011), lentiviruses carrying human *FOXA3*, *HNF1A*, and *GATA4* were introduced into HFF1 cells. However, the expression of hepatic genes was not induced as measured by quantitative PCR (qPCR) (Figure S1C), suggesting that a different protocol is required for hepatic conversion in human cells.

We therefore designed a de novo screen for factors critical for hiHep induction. We selected eight human transcription factors (8TF; Figure 1A; Table S1), including pioneer factors *FOXA3* and *GATA4* (Zaret and Carroll, 2011), liver-enriched transcription factors *HNF1B*, *HNF4A*, *HHEX*, *PROX1*, *C/EBP β* (Zaret, 2008; Zaret and Grompe, 2008), and *KLF4*, a transcription factor important for mesenchymal-to-epithelial transition in reprogramming (Li et al., 2010). The mRNA levels of hepatocyte-specific genes, such as *Albumin (ALB)*, *Cytokeratin 18 (CK18)*, *Transthyretin (TTR)*, and *Transferrin*, were markedly induced in HFF1 after the expression of 8TF (Figure S1D). Upon removing single factors, we found that *FOXA3*, *HNF1B*, and *HNF4A* were important for hepatic conversion (Figures S1E–S1J). Interestingly, replacement of *HNF1B* with *HNF1A*

dramatically enhanced *ALB* expression (Figure S1K). Removing individual factors from *FOXA3*, *HNF1A*, and *HNF4A* (collectively referred to as 3TF) reduced the expression of hepatic genes (Figure 1B). Notably, 3TF induced higher levels of hepatic gene expression than did other combinations of transcription factors (Figure S1L). 3TF also triggered increased H3K9 acetylation at the promoter region of *ALB* and *AAT* genes, suggesting an epigenetic remodeling during hepatic conversion (Figure S1M). Based on these three factors, we improved hiHep induction by optimizing the culture conditions for fibroblasts, fibroblast seeding density, virus infection, and hepatocyte culture medium (see the Supplemental Experimental Procedures; Table S2).

hiHeps induced with 3TF displayed an epithelial morphology at 12 days after induction (Figure 1C). The expression of genes specific for mature hepatocytes, e.g., *ALB*, *ASGPR1*, and *Transferrin*, increased gradually during hiHep induction, suggesting that hepatic conversion is a progressively coordinated process (Figure 1D). By contrast, the expression of fibroblast-specific genes was dramatically reduced in hiHeps (Figure 1E).

hiHeps Possess Gene Expression Pattern and Functions Specific for Mature Hepatocytes

Approximately 20% of cells expressed both *ALB* and α -1-antitrypsin (*AAT*) at day 12 as determined by immunofluorescent staining and flow cytometry (Figures 2A and 2B), suggesting an efficient conversion. Moreover, hiHeps showed a remarkable capability for secreting the plasma proteins *ALB* and *AAT* at the level close to primary human hepatocytes as measured by ELISA (Figures 2C and 2D).

Genome-wide expression profile analysis revealed that hiHeps were clustered closely with cultured PHH (Figure 2E). Expression profiling also showed the fibrotic genes were efficiently silenced in hepatic conversion, which was in line with the published expression profiles of induced pluripotent stem cells (iPSCs) (Sridharan et al., 2009; Stadtfeld et al., 2008). Gene set enrichment analysis (GSEA) showed that pathways enriched in PHHs were significantly enriched in hiHeps, including those involved in lipid metabolism, amino acid metabolism, and phase I and phase II detoxification (Figure S2; Table S3). These data indicate that HFFs undergo hepatic conversion by transcriptional alterations at the whole-genome level. In agreement with the systemic expression of hepatic genes, hiHeps displayed numerous hallmark functions of mature hepatocytes, such as glycogen storage (Figure 2F), acetylated low-density lipoprotein (ac-LDL) intake (Figure 2G), indocyanine

Figure 1. Induction of Hepatocytes from Human Fetal Fibroblasts

(A) Experimental design for the induction of human hepatocytes (hiHeps). Primary human fibroblasts were infected with lentiviruses expressing human hepatic transcription factors (Table S1). The culture medium was changed to HMM medium 2 days after infection. hiHeps were characterized 10–14 days after induction.

(B) *FOXA3*, *HNF1A*, and *HNF4A* induced hepatic gene expression in human fetal limb fibroblasts (HFF1). Withdrawal of individual factors reduced hepatic gene expression as measured by quantitative PCR (qPCR). Data are normalized to 3TF.

(C) hiHeps show typical epithelial morphology.

(D) Gradually increased hepatic gene expression during the induction of hiHeps. The expression levels of the indicated genes were analyzed by qPCR. Data are normalized to HFF+3TF at day 4.

(E) Genes specific to the original fibroblasts were silenced in hiHeps at 2 weeks after induction. Data are normalized to HFF1. PHHs cultured for 2 days were used as controls in (D) and (E).

Scale bars, 100 μ m. Data are represented as the mean \pm SD. See also Figure S1 and Tables S1 and S2.

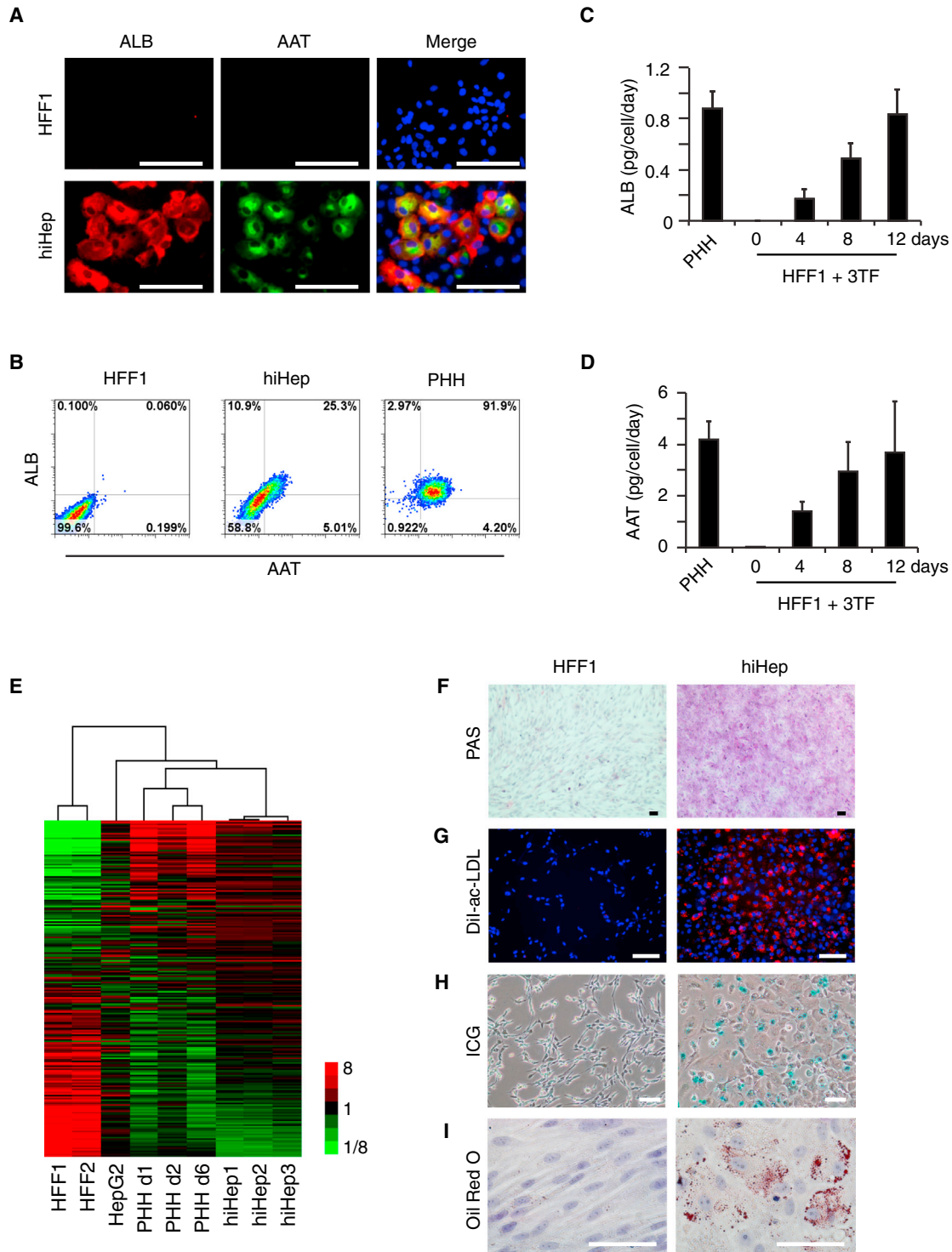


Figure 2. hiHeps Acquire Hepatic Gene Expression Pattern and Mature Functions

(A) Coexpression of the mature hepatic proteins ALB and AAT was determined by immunofluorescent staining. (B) hiHeps were stained for albumin (ALB) and α -1-antitrypsin (AAT) at 2 weeks after induction. ALB and AAT double-positive cells, as quantified by flow cytometry, were used to determine the conversion efficiency of hiHep. PHHs cultured for 2 days were used as positive controls. (C and D) Excretion of ALB (C) and AAT (D) increased during hepatic conversion as measured by ELISA. (E) Gene expression profile analysis of HFFs, PHHs, unsorted hiHeps, and HepG2 cells by cDNA microarray. Hierarchical clustering shows that hiHeps are grouped together with primary human hepatocytes (PHH). PHH were cultured for the indicated number of days. PHH cultured at day 2 were grouped closely to PHH at day 6, suggesting that PHH maintain gene expression at a relatively stable level after cultured for 2 or more days. Human hepatoblastoma cell line HepG2

(legend continued on next page)

green (ICG) absorption (Figure 2H), and cytoplasmic accumulation of neutral triglycerides and lipids (Figure 2I).

Hepatic lineage conversion induced by 3TF was confirmed in an additional HFF cell line, HFF2 (Figures 3A–3D). Furthermore, to exclude the possibility of hepatoblast contamination in fetal cell preparations, we demonstrated that hiHeps could be derived from CD133⁺ EpCAM⁺ fibroblasts (Figure S3).

Additionally, we characterized hepatic conversion from human adult dermal fibroblasts (HAFs). Morphologic change and hepatic gene expression were induced by 3TF in HAFs (Figures 3E and 3F). HAF-derived hiHeps showed hepatic functions, such as glycogen accumulation and ac-LDL intake (Figures 3G and 3H). Intriguingly, less than 10% of the cells were positive for both ALB and AAT (Figure 3I), suggesting that hepatic conversion from HAFs is less efficient than that from HFFs.

Detoxification and Biliary Excretion of hiHeps

Cytochrome P450 (CYP450) enzymes of hepatocytes are major enzymes accounting for drug detoxification. Their activities and responses to specific inducers are irreplaceably used to assess drug metabolism and drug-drug interaction in pharmacology (Guengerich, 2002). Intriguingly, phase I and phase II drug metabolic genes were enriched in both PHH cells and hiHeps (Figure S2; Table S3).

We next analyzed whether hiHeps were responsive to CYP inducers. Before addition of chemical inducers, hiHeps already expressed several CYP450 enzymes at remarkable levels (Figure 4A). Transcriptional activation of CYP450 enzymes and many other drug metabolism enzymes are mediated by nuclear receptors, including AHR, CAR, and PXR (Liddle and Goodwin, 2002). These nuclear receptors were highly expressed in hiHeps as determined by qPCR (Figure 4B). Furthermore, 3-methylcholanthrene, phenobarbital, or rifampicin treatment markedly induced mRNA expression levels of *CYP1A2* (an AHR target gene), *CYP2A6* (a CAR target gene), *CYP2B6*, *CYP2C8*, and *CYP2C9* (target genes of CAR and PXR). *CYP3A4*, which is a target gene of CAR and PXR, was induced at a relatively low but significant level by phenobarbital (Figure 4C). Importantly, in another assay for CYP activities, hiHeps showed CYP enzyme-dependent metabolism of phenacetin, coumarin, and dextromethorphan (Figure 4D).

Membrane transporter-mediated biliary excretion is another important function of hepatocytes for clearance of xenobiotics. Drug clearance through biliary excretion is a critically evaluated property in the selection of drug candidates (Liu et al., 1999; Pan et al., 2012). Significant efforts have been made to identify surrogate in vitro models to evaluate biliary excretion (Liu et al., 1999; Pan et al., 2012). We found that the expression levels of key transporter genes were significantly expressed in hiHeps (Figure 4E). Importantly, hiHeps

showed remarkable biliary excretion indices (BEI) for the clearance of multiple efflux transporter substrates, such as [D-Pen2,5]-enkephalin hydrate (DPDPE), D8-taurocholic acid (D8-TCA), and cholesteryl-luciferin (CLF) (Figure 4F), suggesting a potential application for hiHeps in the assessment of drug biliary clearance. Together, our data indicate that hiHeps possess remarkable mature hepatic phenotypes and functions.

Expansion of Functional hiHeps by SV40 Large T Antigen

For in vivo functional characterization, it is necessary to expand hiHeps in large numbers. However, hiHeps derived from both HFFs and HAFs were proliferation arrested (Figure 5A), likely caused by reduced expression of Cyclin A and B (Figure S4A). After employing several strategies, we found that the Lentivirus-mediated expression of SV40 large T antigen (LT) allowed hiHeps to proliferate with restored expression of Cyclin A and B (Figure 5A; Figure S4B). hiHeps with LT expression (hiHep^{LT}) exhibited typical epithelial cell morphology (Figure 5B) and expressed mature hepatic genes at the levels comparable to those in hiHeps, e.g., *ASGPR1* and *Transferrin* (Figures 5B and 5C). Expression profile analysis revealed that hiHep^{LT} cells were clustered together with hiHeps and PHH (Figure 5D). Moreover, hiHep^{LT} cells acquired mature hepatic functions, including glycogen accumulation, ac-LDL absorption, ALB secretion, CYP metabolism, and biliary excretion (Figures 5E–5J). Compared with hiHeps, hiHep^{LT} cells showed similar biliary excretion functions, whereas albumin secretion and CYP activities were attenuated (Figures 5G–5J). Remarkably, hiHep^{LT} cells maintained constant levels of hepatic gene expression and functions after several passages (Figures 5C–5F). Similarly, hiHep^{LT} cells were successfully induced from HAFs (Figures S4C–S4E). Furthermore, we generated hiHeps from adipose tissue-derived mesenchymal stem cells (AD-MSC), which are readily available from patients. hiHeps derived from AD-MSCs possessed comparable hepatic functions to those of fibroblast-derived hiHeps (Figures S4F–S4J).

hiHeps Are Stably Converted Mature Hepatocytes but Not Hepatic Progenitor Cells

Notably, exogenous *FOXA3*, *HNF1A*, and *HNF4A* were silenced in expandable hiHeps (Figure S5A), whereas endogenous factors were markedly induced (Figure S5B). These data suggest stable conversion of hiHeps to a hepatic fate. Although hiHep^{LT} cells were proliferating cells, hepatoblast marker genes, including *EpCAM*, *DLK1*, *LGR5*, and *CYP3A7*, were undetectable or expressed at low levels (Figures S5C and S5D). A low level of α -fetoprotein (*AFP*) mRNA was detected in hiHep^{LT}, which is slightly higher than that observed in human liver cells

was included to reveal that the expression pattern of hiHeps is closer to that of PHH as indicated by the cluster tree on the top. Expression levels are depicted in colors.

(F) Glycogen storage by hiHeps was confirmed by periodic acid-Schiff (PAS) staining (magenta).

(G) Intake of acetylated low density lipoprotein labeled with the fluorescent probe 1,1'-dioctadecyl-3,3',3'-tetramethyl-indocarbocyanine perchlorate (DiI-ac-LDL) in hiHeps (red).

(H) Indocyanine green (ICG) uptake in hiHeps (green).

(I) Lipid accumulation in hiHeps as shown by oil red O staining.

Scale bars, 100 μ m. Data are represented as the mean \pm SD. See also Figure S2 and Table S3.

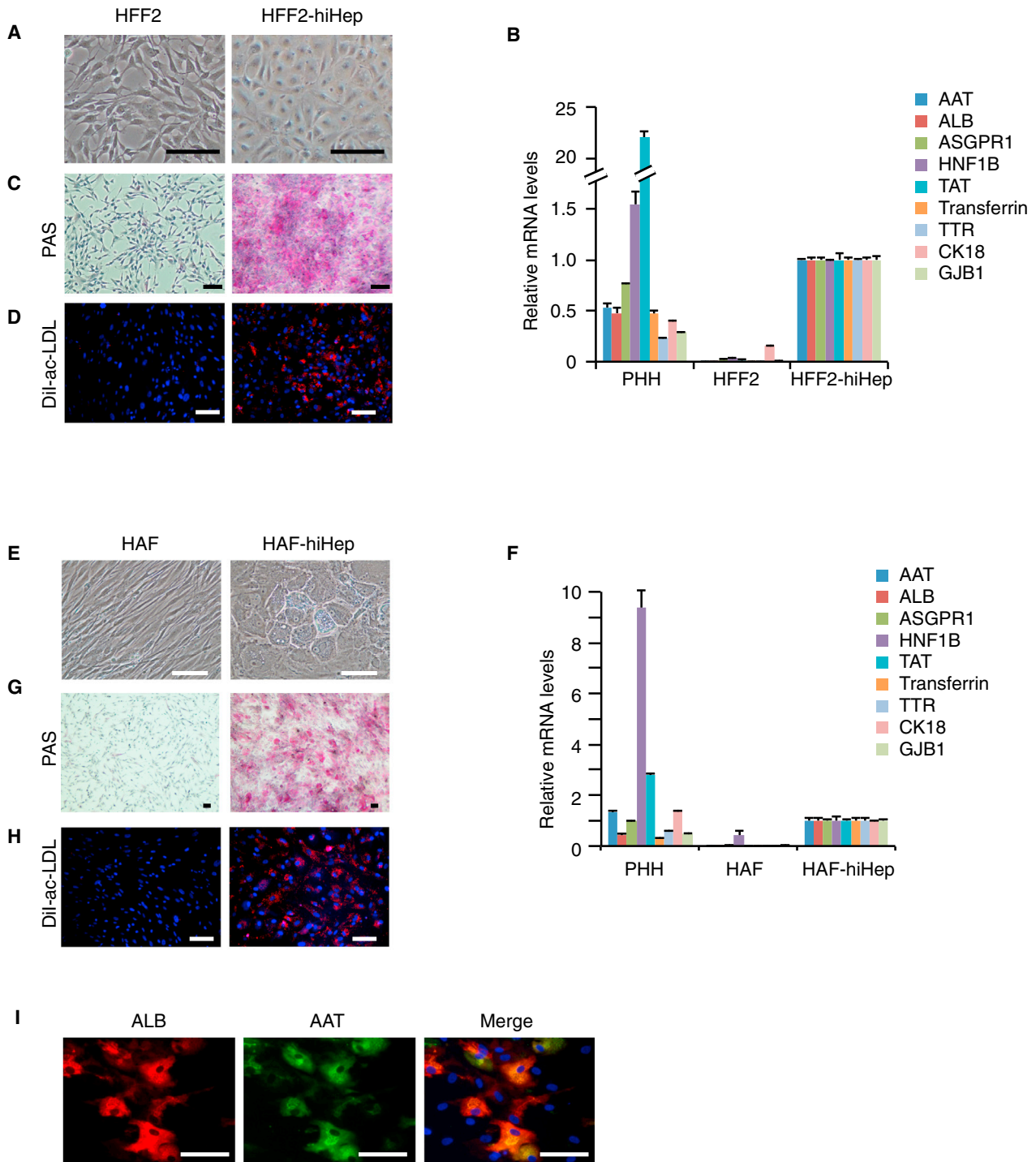


Figure 3. Generation of hiHeps from Human Fetal and Adult Fibroblasts

(A) hiHeps derived from another fetal fibroblast line, HFF2, by FOXA3, HNF1A, and HNF4A overexpression exhibited epithelial-like morphology. (B) HFF2-derived hiHeps expressed hepatic genes as determined by qPCR. PHHs cultured for 2 days were used as controls. Data are normalized to HFF2-hiHep. (C and D) HFF2-derived hiHeps exhibited hepatic functions, including glycogen storage, as determined by PAS staining (C) and ac-LDL intake (D). (E) hiHeps derived from human adult fibroblasts (HAFs) exhibited epithelial-like morphology. (F) Hepatic gene expression induced by 3TF in HAF-derived hiHeps as measured by qPCR. PHHs cultured for 2 days were used as controls. Data are normalized to HAF-hiHep. (G and H) HAF-derived hiHeps exhibited hepatic functions, including glycogen storage, as determined by PAS staining (G) and ac-LDL intake (H). (I) Twelve days after hepatic induction in HAFs, 10% of the cells expressed both ALB and AAT as determined by immunofluorescent staining. Scale bars, 100 μ m. Data are represented as the mean \pm SD. See also Figure S3.

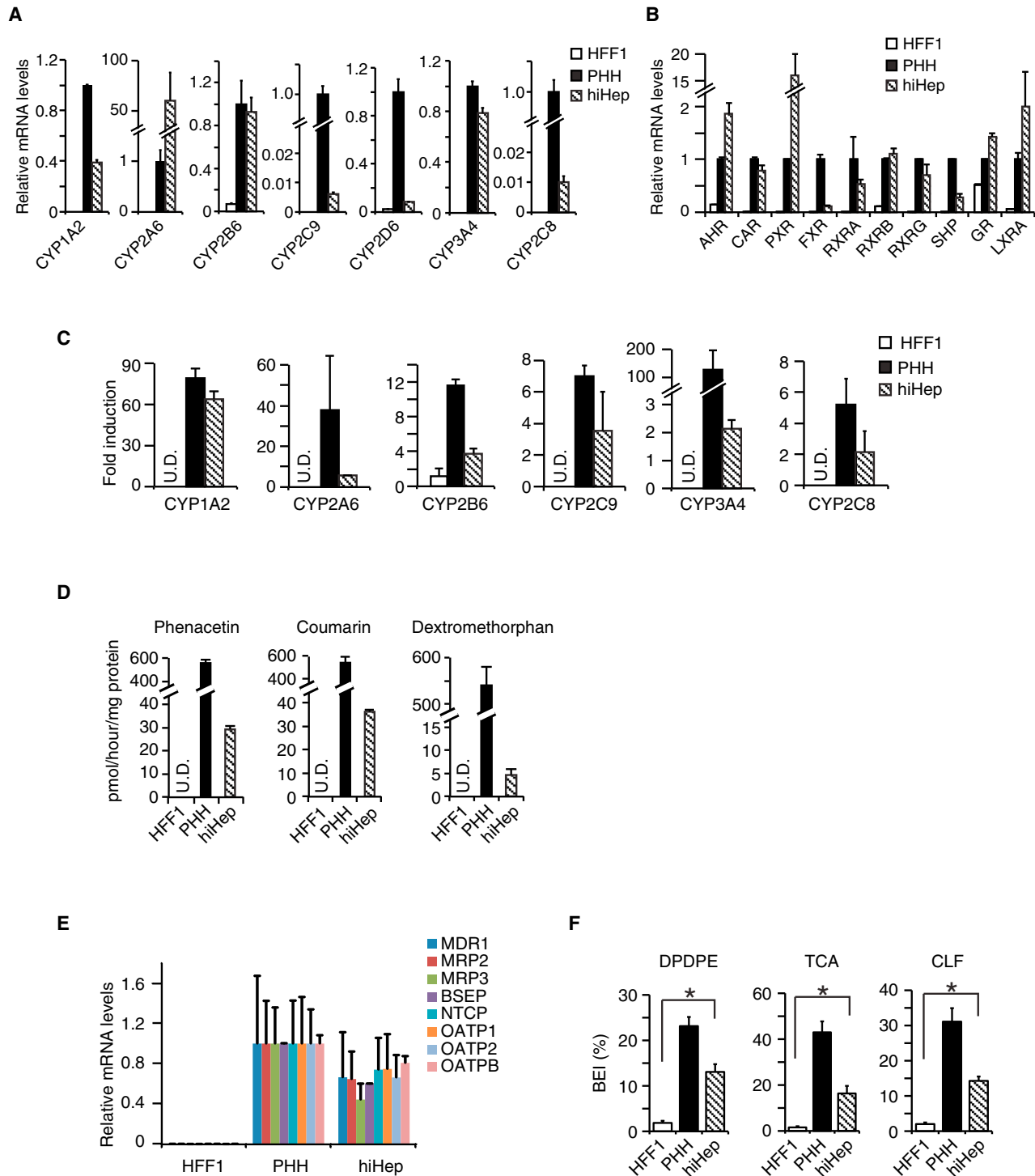


Figure 4. hiHeps Possess CYP Enzyme Activities and Biliary Excretion Capability

(A–C) For the measurement of Cytochrome P450 (CYP) enzyme expression and induction, hiHeps and PHHs were cultured for 48 hr and then changed to medium supplemented with or without chemical inducers for additional 48 hr.

(A) The mRNA levels of CYP genes were determined by qPCR in PHHs and hiHeps cultured for 2 days before inducer treatment. Data are normalized to PHH.

(B) Expression levels of detoxification-related nuclear receptors were measured by qPCR in hiHep, and PHH cells were cultured for the same duration as in (A). Data are normalized to PHH.

(C) The mRNA levels of the induced CYP enzymes were measured by qPCR. CYP1A2 was induced by 3-methylcholanthrene. CYP2A6, CYP2C8, and CYP2C9 were induced by rifampicin. CYP2B6 and CYP3A4 were induced by phenobarbital. Fold induction in hiHep and PHH cells were normalized to the levels in cells without inducer treatment, respectively.

(legend continued on next page)

(Figure S5E). The AFP protein level in hiHep^{LT} cells was undetectable by immunofluorescent staining (Figure S5F). Furthermore, hepatoblast marker genes, including *TBX3* and *SOX9*, were not induced during the early stage of hepatic lineage conversion (Figure S5G). Importantly, biliary epithelium marker genes were not expressed in hiHep^{LT} cells, and hiHep^{LT} cells did not develop bile duct tubes in a three-dimensional culture (Figures S5H and S5I). These results largely exclude the existence of bipotential hepatic progenitors in hiHeps. Taken together, our results indicate that hiHeps are mature hepatocytes, but not hepatoblasts.

hiHep Transplantation Improves Fah-Deficiency-Induced Liver Metabolic Disease

The expansion of hiHep^{LT} cells in large numbers allowed the measurement of hepatic functions in vivo. We transplanted hiHep^{LT} cells into fumarylacetoacetate hydrolase-deficient (*Fah*^{-/-}) mice (Azuma et al., 2007; Overturf et al., 1996). *Fah*^{-/-} mice were maintained with 2-(2-nitro-4-trifluoro-methylbenzyl)-1,3-cyclohexanedione (NTBC) supply and died of liver failure within 4–6 weeks after NTBC withdrawal (Azuma et al., 2007; Overturf et al., 1996). Wild-type hepatocytes can repopulate the liver and rescue *Fah*^{-/-} mice after intrasplenic transplantation, thus providing a useful model to characterize the in vivo function of hiHeps.

To reduce the immunological response to human cells, *Fah*^{-/-}*Rag2*^{-/-} (F/R) mice lacking mature T and B cells were additionally treated with antibodies against mouse asialo-GM1, which depleted NK-cells, and the immunosuppressive drug FK506 (Figure 6A) (He et al., 2010). F/R mice that did not receive transplanted cells and those that were transplanted with HFF cells lost their body weights and died approximately 4 weeks after removing the supply of NTBC (Figure 6B), whereas transplantation with PHH extended the life of F/R mice (Figure 6B, 3 of 8 mice survived). Notably, 5 of 15 recipient mice survived 9 weeks after transplantation with hiHep^{LT} cells (Figure 6B). The mice transplanted with PHH and hiHep^{LT} cells lost their body weights during the first 3 weeks but regained or stabilized their body weights in the rest period of the experiment (Figure S6A). Serum levels of ALT and AST were significantly reduced in the surviving recipients (Figures 6C and 6D), suggesting that the liver functions improved. Human ALB was also detected in the sera of mice transplanted with hiHep^{LT} cells (Figure 6E).

Immunohistochemical staining of human *Fah* and *AAT* showed that hiHep^{LT} cells repopulated 0.3%–4.2% of the liver parenchyma in the surviving mice (Figures 6F, S6B, and S6C). Repopulated *Fah*-positive cells were positively stained by HepPar-1, an antibody specifically labeling human hepatocytes, but not mouse hepatocytes or nonhepatic cells (Figure S6D). Engraftment of hiHep^{LT} cells in recipient livers was further confirmed by genomic PCR for human-specific Alu DNA sequences (Fig-

ure 6G). Notably, hiHeps did not fuse with mouse hepatocytes as determined by immunofluorescent staining using antibodies specifically against *FAH* and mouse Albumin (Figure S6E). Repopulated hiHep^{LT} cells were microdissected for analysis of human hepatic gene expression. Compared with cultured hiHep^{LT} cells, the mRNA levels of human *ALB* and *AAT* were attenuated in repopulated hiHep^{LT} cells, whereas the expression of *CYP3A4* was increased (Figure 6H). Remarkably, AFP levels were further reduced in repopulated hiHep^{LT} cells (Figure 6I), suggesting that the gene expression pattern of hiHep^{LT} is further remodeled by the in vivo microenvironment. Together, our data suggest that hiHep^{LT} cells can repopulate F/R livers and ameliorate impaired liver functions caused by *Fah* deficiency.

In this experimental setting, SV40 LT was merely employed as a strategy to expand hiHeps for in vivo functional assays. Nevertheless, we characterized the tumorigenicity of hiHep^{LT} cells. Intriguingly, tumors were not detected in recipient F/R mice (data not shown). Repopulated hiHep nodules were not proliferating as shown by Ki67 staining 9 weeks after transplantation (Figure S6D), likely due to attenuated SV40 LT expression in vivo (Figure S6F). Moreover, we found that hiHep^{LT} cells maintained normal chromosome numbers at late passages (Figure S6G) and did not form tumors after transplantation in immunodeficient mice (Figure S6H).

hiHeps Improve Con-A-Induced Fulminant Liver Failure

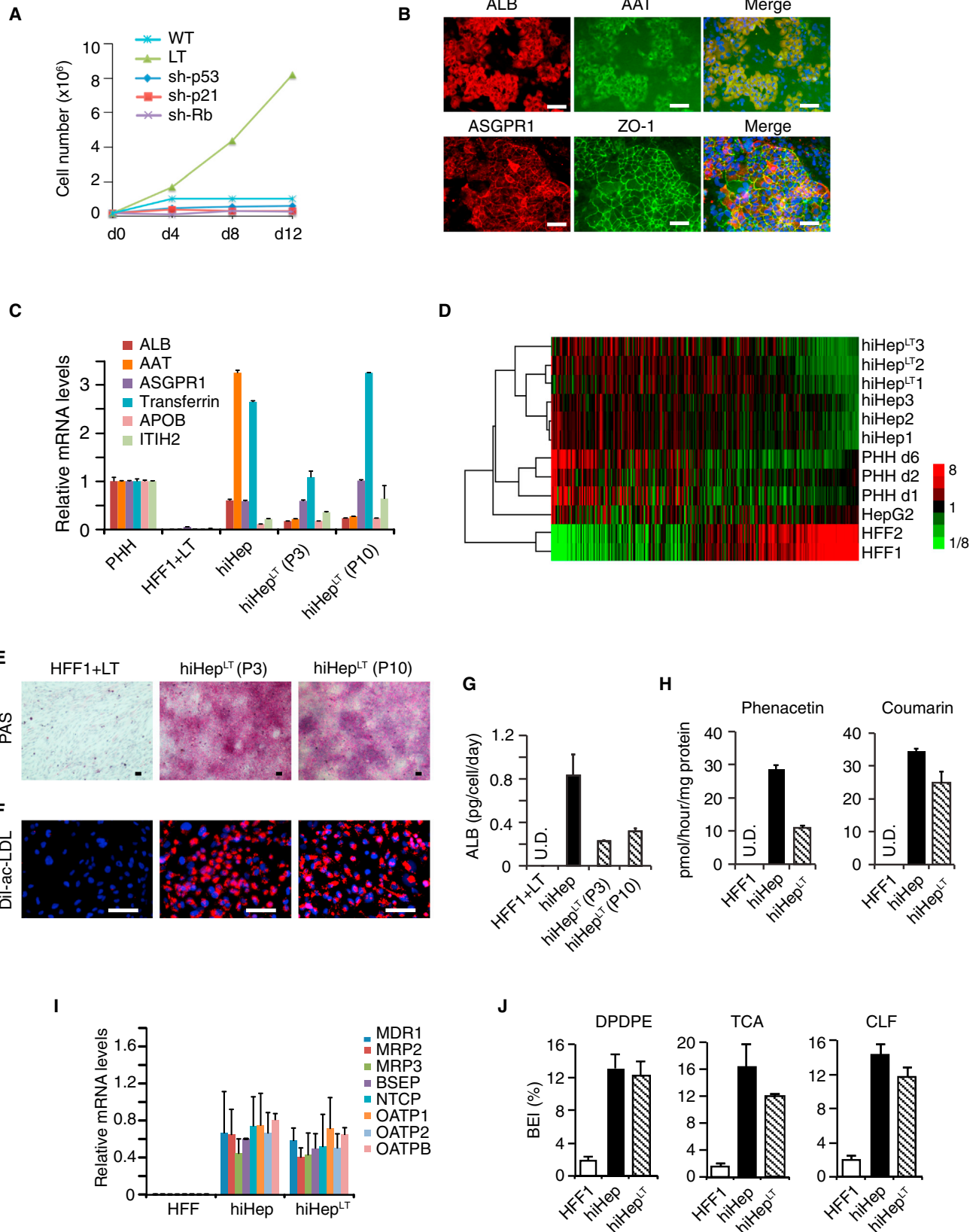
Encouraged by these results, we determined whether hiHeps could have sufficient hepatic functions to support liver in recovering from fulminant hepatitis. To that end, wild-type mice were injected with concanavalin A (Con A) to trigger fulminate hepatitis and animal death within 12–24 hr (Figures 7A and 7B) (Tiegs et al., 1992). As an experimental model to demonstrate hepatic functions of hiHeps, we encapsulated hiHep^{LT} cells in alginate-poly-L-lysine-alginate (APA) microcapsules (Figure S7A) and intraperitoneally injected encapsulated cells into acute liver failure mice (Figure 7A). Previous studies have shown that transplantation of APA-encapsulated primary hepatocytes improved the survival of animals with acute liver failure (Mei et al., 2009; Roger et al., 1998; Wong and Chang, 1986). Semi-permeable APA microcapsules isolate encapsulated cells from the immune cells in the recipient but allow the exchange of molecules smaller than 100 kDa (Orive et al., 2004; Wang et al., 2006; Xie et al., 2011). As a confirmation of the semipermeability, human ALB was readily detected in the serum of recipient mice after intraperitoneal transplantation of APA-encapsulated hiHep^{LT} cells (Figures S7B).

Encapsulated cells were injected intraperitoneally into wild-type mice 8 hr after Con A treatment (Figure 7A). In groups transplanted with encapsulated HFFs and HepG2, almost all recipients died within 24 hr after Con A treatment (one mouse in the HFF group died at day 3, Figure 7B; Movie S1). PHH

(D) CYP metabolic activity in hiHeps. CYP enzymes were induced in hiHeps for 48 hr. Freshly thawed primary human hepatocytes were directly used as a positive control. The metabolic products of phenacetin (acetaminophen, assay for CYP1A2 activities), coumarin (7-hydroxycoumarin, assay for CYP2A activities), and dextromethorphan (dextrorphan, assay for CYP2D6 activities) were determined by liquid chromatography-tandem mass spectrometry. U.D., undetectable.

(E) Expression of drug transporter genes in hiHeps as determined by qPCR. Data are normalized to PHH.

(F) hiHeps show the capability for biliary excretion as measured by clearance of [D-Pen2,5]-enkephalin hydrate (DPDPE), D8-taurocholic acid (D8-TCA), and choly-l-lysyl-fluorescein (CLF). Sandwich cultured PHH were used as positive controls. **p* < 0.05, *t* test. Data are represented as the mean ± SD.



(legend on next page)

treatment significantly improved the survival rate and extended the survival time of mice with acute liver failure (Figure 7B). Markedly, upon treatment with encapsulated hiHep^{LT} cells, 5 of 14 mice completely recovered from Con-A-induced acute liver failure (Figure 7B; Movie S2) and showed normal serum ALT and AST levels 4 days after Con A treatment (Figures 7C, 7D, and S7C). It is worth noting that HepG2 cells have been used in previous models of bioartificial liver-supporting devices; however, HepG2 cells showed no therapeutic effect on acute liver failure in mice, suggesting that hiHeps may hold promise for the development of the next generation of bioartificial liver-supporting devices. Histological analysis revealed that encapsulated hiHep^{LT} cells significantly improved recovery from Con-A-induced liver damage (Figures 7E and 7F). Together, these results reveal the hepatic functions of hiHeps in vivo and provide evidence for the therapeutic effect of hiHeps in the treatment of liver injuries, such as metabolic liver disease and acute liver failure.

DISCUSSION

Here, we have generated functionally mature human hepatocytes directly from fibroblasts. Consistent with previous studies on lineage conversion, our results show that human cells are resistant to reprogramming, and multiple optimizations were applied to develop a strategy for efficient hiHep induction (see the Supplemental Experimental Procedures; Table S2). hiHeps were induced by a set of factors: *FOXA3*, *HNF1A*, and *HNF4A*. Intriguingly, it is known that *HNF4A* activates the *HNF1A* promoter (Kuo et al., 1992), and *Hnf4a* alone with *Foxa1*, 2, or 3 are sufficient to induce mouse iHeps (Sekiya and Suzuki, 2011). However, additional expression of *HNF1A* is necessary for conversion of human fibroblasts. This may be partially explained by the fact that the transcriptional binding sites and regulation differ in human and mouse liver cells (Odom et al., 2007), despite the fact that these factors are essential for hepatic gene expression in both human and mouse cells (Zaret and Carroll, 2011). We also found that the removal of *C/EBPβ* and *GATA4* enhanced hepatic gene expression. During the induction of hiHeps, the exogenous transcription factors trigger a dynamic change of cell identity. This process is different from the static cell identity of mature hepatocytes or liver development. It is likely that during hepatic conversion

the specific combination of transcription factors form a regulatory network distinctive from that in hepatocytes. It is thus possible that the roles of *C/EBPβ* and *GATA4* in hepatic conversion are dependent on the specific combination of factors used for hiHep induction.

Proliferation arrest is a major hurdle for the application of terminally differentiated cells generated by forced lineage change (Graf and Enver, 2009). We previously used *p19Arf* inactivation to expand mouse iHeps (Huang et al., 2011), which was insufficient for human cells. This is likely due to the difference between the two species, because the inactivation of *p53* alone was able to immortalize mouse fibroblasts (Harvey et al., 1993; Tsukada et al., 1993) but was not enough to enhance proliferation of human cells in vitro (Kiyono et al., 1998; Shay et al., 1991). We found that LT expression enabled hiHeps to proliferate. ALB- and AAT-expressing cell numbers were increased in hiHep^{LT} cells, likely resulting from continuous lineage conversion during proliferation of these cells (Hanna et al., 2009). hiHep^{LT} cells provided us the opportunity to definitively demonstrate the therapeutic effects of hiHeps on metabolic liver disease and acute liver failure. Moreover, repopulation of hiHeps in Fah-deficient mice presents a strategy for development of humanized animal models for biomedical research. Intriguingly, hiHep^{LT} cells appeared to be nontumorigenic, partially due to attenuated SV40 LT levels in hiHep^{LT} cells after transplantation in mice. Also, this observation is in line with previous findings that SV40 LT alone is not sufficient to induce tumorigenesis in mammalian cells (Land et al., 1983). Although the expression of LT in hiHeps is not a concern for in vitro disease modeling and application in extracorporeal bioartificial liver-supporting devices (Carpentier et al., 2009), a controllable LT expression system or other safe measures to expand hiHeps should be developed for cell replacement therapies.

Patient-derived hiHeps represent a type of functional hepatocytes that could be used in personalized regenerative medicine and disease modeling. This is an advantage unmatched by HepG2 or other hepatic cell lines (Castell et al., 2006). Previous studies have successfully generated hepatocytes from human iPSCs (Ji et al., 2013). The derivations of hepatocytes from iPSCs or direct lineage conversion represent two valuable approaches to obtain surrogate hepatocytes for disease modeling and therapeutic applications.

Figure 5. Expanding hiHeps

(A) hiHeps are proliferation arrested. Knockdown of p53, p21, or Rb had minimal effects on the proliferation of hiHeps; however, SV40 large T antigen endows hiHeps with proliferative capability. HFF1 cells were transduced with SV40 large T antigen (HFF1+LT), followed by 3TF overexpression to induce hepatic conversion (hiHep^{LT}).

(B) Expandable hiHep^{LT} cells displayed typical epithelial morphology and expressed hepatic proteins specific for mature hepatocytes as shown by coimmunostaining of ALB and AAT (top panel) and ASGPR1 and ZO-1 (bottom panel).

(C) hiHep^{LT} at early (passage 3) and late (passage 10) passages show similar expression levels of hepatic genes as determined by qPCR. PHHs cultured for 2 days were used as controls. Data are normalized to PHH.

(D) Whole-genome expression analysis shows that the expression pattern of hiHep^{LT} cells is clustered with that of hiHeps and primary human hepatocytes (PHH).

(E–G) hiHep^{LT} cells at early and late passages show comparable glycogen accumulation (PAS staining) (E), Dil-ac-LDL intake (F), and ALB secretion (G).

(H) CYP metabolic activities of hiHep^{LT} cells at passage 10. The products of phenacetin and coumarin metabolism were determined by liquid chromatography-tandem mass spectrometry. The products of dextromethorphan metabolism were not detected in hiHep^{LT} cells.

(I) A qPCR assay shows that hiHep^{LT} cells express high levels of drug transporter genes.

(J) hiHep^{LT} cells at passage 10 show a biliary excretion capability comparable to that of hiHeps.

Scale bars, 100 μm. Data are represented as the mean ± SD. See also Figures S4 and S5.

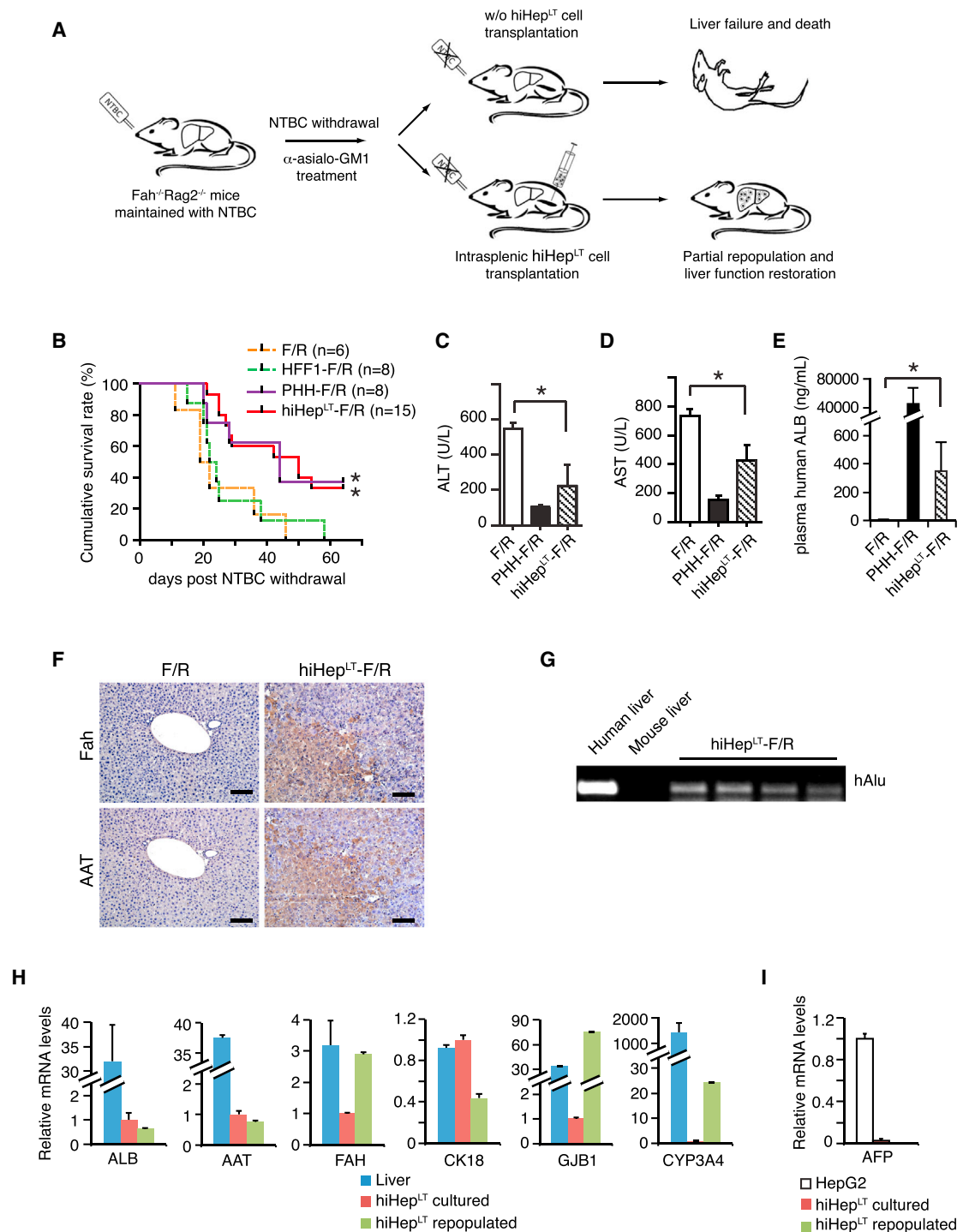


Figure 6. The Therapeutic Effects of hiHeps on Metabolic Liver Diseases

(A) Schematic outline of hiHep^{LT} cell transplantation into the livers of Fah^{-/-}Rag2^{-/-} mice (F/R). NTBC was withdrawn from drinking water before cell transplantation. F/R mice were pretreated with an antibody against asialo-GM1 1 day before cell transplantation to deplete natural killer cells. HFF1 (1 × 10⁷ cells), hiHep^{LT} (1 × 10⁷ cells), or PHH (1 × 10⁶ cells) were intrasplenically transplanted into F/R mice. To reduce immunerejection of the donor cells, the recipient mice were administered anti-mouse asialo-GM1 at 7 day intervals and were given the immunosuppressive drug FK506 daily. Animals were monitored daily and sacrificed 9 weeks after transplantation.

(B) Kaplan-Meier survival curve of F/R mice that did not receive cells or received 1 × 10⁷ HFF1 (HFF-F/R), hiHep^{LT} (hiHep^{LT}-F/R) or 1 × 10⁶ PHH (PHH-F/R) after NTBC withdrawal.

(C and D) Serum levels of ALT (C) and AST (D) in moribund control F/R mice (n = 3), surviving hiHep^{LT}-F/R mice (n = 5), and surviving PHH-F/R mice (n = 3).

(E) Human ALB levels were determined by ELISA in the sera of surviving hiHep^{LT}-F/R and PHH-F/R mice.

(legend continued on next page)

Our data show that hiHeps resemble PHH markedly in terms of gene expression, hepatic functions, and therapeutic effects; therefore, hiHeps have potential uses as surrogate hepatocytes in pharmaceutical research and cellular therapies (Ji et al., 2013; Yu et al., 2012). For example, biliary excretion is a key function of mature hepatocytes for the detoxification of nondegradable xenobiotics (Pan et al., 2012). Because hiHeps possess significant biliary excretion functions, it is possible to apply these cells in evaluating biliary excretion of candidate drugs.

It is remarkable that the repopulation of hiHeps rescued around 30% of Fah-deficient mice. Previous studies have shown that transplantation of primary mouse hepatocytes usually leads to a survival rate close to 100% (Huang et al., 2011), whereas a survival rate of 30%–50% is commonly observed after transplantation of human primary hepatocytes (He et al., 2010). Interestingly, the serum albumin level in hiHep-transplanted mice was only 1/20–1/30 of that in PHH-transplanted mice when normalized to the repopulation efficiency. Therefore, it is plausible that there may be therapeutic effects of hiHeps or primary hepatocytes other than secretion of Albumin. Nevertheless, the function of hiHeps needs further improvement in order to obtain better therapeutic effect or to generate humanized animal models. On the other hand, because encapsulated hiHeps show the capability to treat acute liver failure mice, it would be of great interest to determine whether hiHeps could be used as source cells for extracorporeal bioartificial liver-supporting devices in the future (Palakkan et al., 2013).

EXPERIMENTAL PROCEDURES

Detailed Experimental Procedures are provided in the [Supplemental Experimental Procedures](#).

Lentivirus Production

Modified pWPI plasmids carrying candidate genes were introduced into 293FT cells together with packaging plasmid psPAX2 (Addgene) and envelop plasmid pMD2.G (Addgene) to produce viruses.

hiHep Induction and Cell Culture

Human fibroblasts were seeded on a collagen-I-coated dish and infected with lentiviruses carrying the indicated genes. Human fetal fibroblasts (HFFs) and human adult fibroblasts (HAFs) were cultured in human fibroblast medium (HFM). HFF1 and HFF2 were derived from limbs of human fetuses. HAFs were derived from human skin biopsy. Primary human hepatocytes were purchased from Invitrogen GIBCO or Celsis In Vitro Technologies. Institutional ethical committees approved collection and use of human samples.

Human Albumin and α -1-Antitrypsin ELISA

Human Albumin and α -1 Antitrypsin were measured by the human Albumin ELISA Quantitation Set (Bethyl Laboratory) and the human α -1-Antitrypsin ELISA kit (Bethyl Laboratory).

Microarray Analysis

Total RNAs were hybridized to whole-human gene expression microarray (Agilent) in accordance with the manufacturer's instruction. Data were normal-

ized using Gene-Spring (Agilent). Original data are available in the NCBI Gene Expression Omnibus (accession number GSE42643).

Assays for PAS, ac-LDL, ICG, and Oil Red O Staining

Cells were stained by Periodic-Acid-Schiff (PAS, Sigma-Aldrich) and Dil-ac-LDL (Invitrogen). For indocyanine green (ICG, Sigma-Aldrich) uptake assay, cells were changed medium with 1 mg/ml ICG and incubated at 37°C for 1 hr, followed by washing with PBS three times. For oil red O staining, confluent cells were stained by oil red O (Sigma-Aldrich).

CYP Metabolism Assay

For the measurement of CYP enzyme activities, cells were induced with different compounds for certain drug metabolisms. The supernatants were collected for measurement of metabolized compounds by liquid chromatography-tandem mass spectrometry (LC-MS/MS; Agilent 1200 HPLC and ABI 4000 mass spectrometer).

Biliary Excretion Assay

Cells were incubated with test compound solution (DPDPE 5 μ M, CLF 2.5 μ M, and D8-TCA 5 μ M and diluted in Hank's balanced salt solution [HBSS] buffer). DPDPE and D8-TCA were analyzed by LC-MS/MS (LCMS-8030; Shimadzu). The amount of CLF was quantified by measuring fluorescence at 492 and 536 nm with a Synergy 4 microplate reader (Biotek). Biliary excretion index (BEI) was calculated as $BEI = (AHBSS - AHBSS(Ca^{2+} \text{ free})) / AHBSS \times 100\%$.

Transplantation of hiHep^{LT} Cells into Fah-Deficient Mice

All animal experiments were performed in accordance with institutional regulations. hiHep^{LT} cells were intrasplenically transplanted into F/R mice after the withdraw of NTBC water. Body weight was monitored twice a week posttransplantation. Surviving recipient mice were sacrificed to collect blood and liver samples 9 weeks after transplantation.

hiHep^{LT} Cell Transplantation to Concanavalin-A-Induced Acute Liver Failure Mice

C57Bl6/J mice were injected with concanavalin A (Sigma-Aldrich) at the dose of 37.5 mg per kg body weight through tail vein. Encapsulated HFFs, hiHep^{LT} cells, or PHH were injected intraperitoneally into acute liver failure mice. Blood samples were collected from surviving mice in a 24 hr interval. Liver samples were collected after the surviving animals were sacrificed. All animal experiments were performed in accordance with institutional animal regulations.

Statistics

For most statistic evaluation, unpaired Student's t test was applied for calculating statistical probability in this study. For survival analysis, the Mantel-Cox log rank test was applied. Statistic calculation was performed using Statistical Program for Social Sciences software (SPSS, IBM). For all statistics, data from at least three independent samples or repeated experiments were used.

ACCESSION NUMBERS

The microarray data reported in this paper has been deposited in the NCBI GEO under accession number GSE42643.

SUPPLEMENTAL INFORMATION

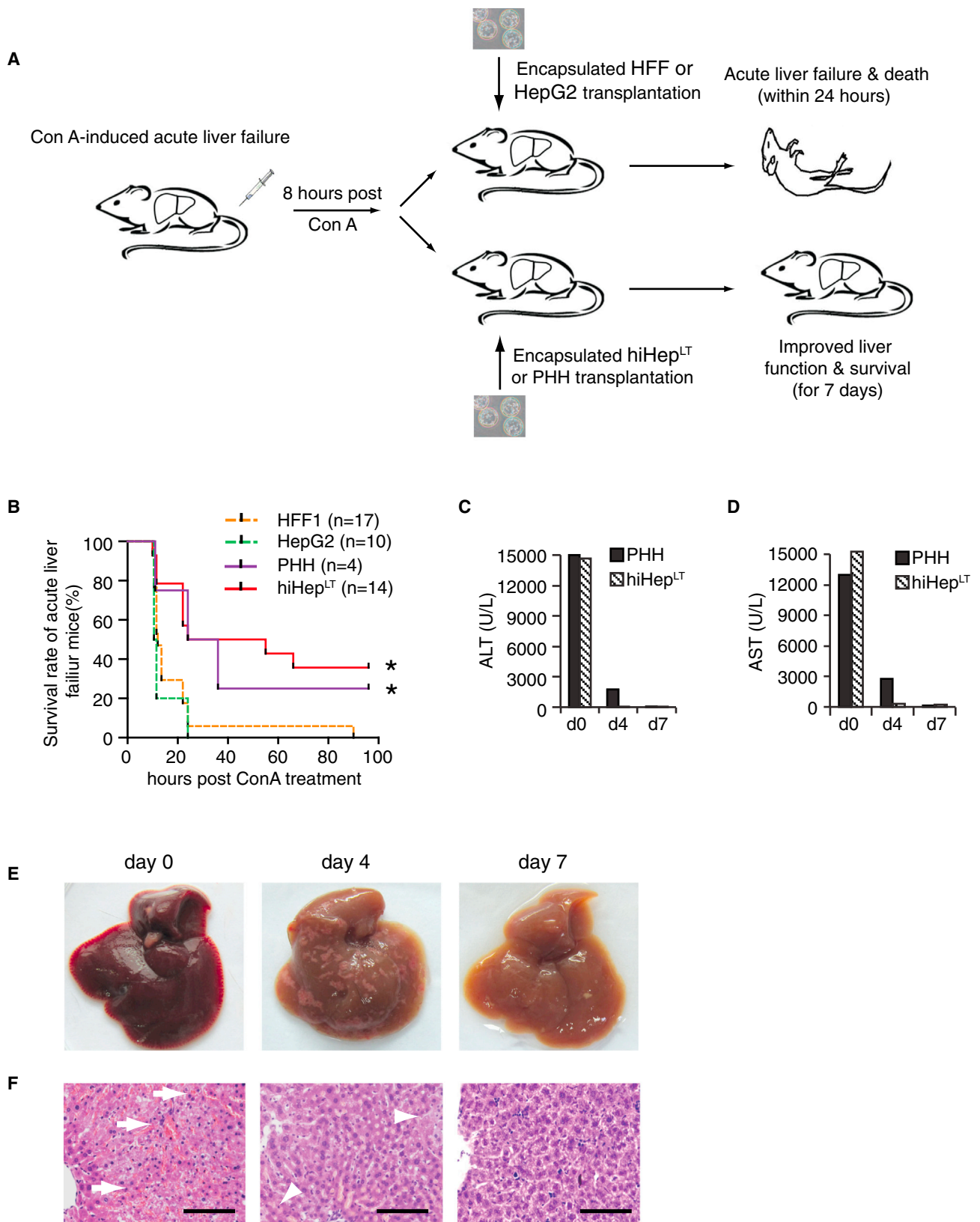
Supplemental Information includes Supplemental Experimental Procedures, seven figures, four tables (All PCR primers were provided in Table S4), and two movies and can be found with this article online at <http://dx.doi.org/10.1016/j.stem.2014.01.003>.

(F) The integration of hiHep^{LT} cells in F/R livers was determined by immunostaining for human Fah and AAT in serial sections.

(G) Human-specific Alu sequences were analyzed by PCR using genomic DNA extracted from hiHep^{LT}-repopulated F/R livers.

(H and I) Fah-positive hiHep^{LT} cells were collected by laser-capture microdissection from serial liver sections. The mRNA levels of the indicated genes were measured in hiHep^{LT}-repopulated nodules (hiHep^{LT} repopulated) and in cultured hiHep^{LT} cells (hiHep^{LT} cultured) by qPCR. Data are normalized to cultured hiHep^{LT} cells (H). mRNA levels of AFP are normalized to that in HepG2 cells (I).

* $p < 0.05$, log rank test for (B) and t test for (C)–(E). Scale bars, 100 μ m. Data are represented as the mean \pm SD. See also [Figure S6](#) and [Table S4](#).



(legend on next page)

AUTHOR CONTRIBUTIONS

L.H. conceived the study and wrote the manuscript. P.H. and Y.G. performed the in vitro experiments. L.Z. performed the in vivo characterization. L.Z., X. Chen, X. Cheng, D.L., and Z. Hu assisted with hiHep generation and characterization. D.Y., Z.W., and G.P. determined the biliary excretion capability. Z. He, J.C., C.L., Y.H., and X.W. performed the transplantation into Fah-deficient mice and analyzed the results of this experiment. Y.Z., L.C., J.C., and X.M. performed the transplantation of encapsulated cells and analyzed the results of this experiment. X.W., Z. He, G.P., X. Cheng, P.H., L.Z., and Y.G. were involved in manuscript preparation.

ACKNOWLEDGMENTS

We thank Dr. Dangsheng Li for critical suggestions during the manuscript preparation and Min Du and Dr. Yuan Ji for support on histological analysis. The L.H. laboratory is funded by the Chinese Academy of Sciences (CAS; XDA01030301 and XDA01020308), the Ministry of Science and Technology (MOST) of China (2012CB945001), and the National Science Foundation of China (NSFC; 913193023 and 31225016). The X.W. laboratory is funded by the MOST of China (2011CB966200) and the NSFC (31271469, 31271474, and 31271042). The G.P. laboratory is supported by the NSFC (81302836), by the MOST (2012ZX09301001-006, 2012ZX09302003), and by the CAS (the Hundred Talents Program). The X.M. laboratory is supported by the NSFC (21076207 and 81101757) and by the CAS (XDA01030303).

Received: August 2, 2013

Revised: November 7, 2013

Accepted: January 2, 2014

Published: February 27, 2014

REFERENCES

- Azuma, H., Paulk, N., Ranade, A., Dorrell, C., Al-Dhalimy, M., Ellis, E., Strom, S., Kay, M.A., Finegold, M., and Grompe, M. (2007). Robust expansion of human hepatocytes in Fah^{-/-}/Rag2^{-/-}/Il2rg^{-/-} mice. *Nat. Biotechnol.* **25**, 903–910.
- Carpentier, B., Gautier, A., and Legallais, C. (2009). Artificial and bioartificial liver devices: present and future. *Gut* **58**, 1690–1702.
- Castell, J.V., Jover, R., Martínez-Jiménez, C.P., and Gómez-Lechón, M.J. (2006). Hepatocyte cell lines: their use, scope and limitations in drug metabolism studies. *Expert Opin. Drug Metab. Toxicol.* **2**, 183–212.
- Cherry, A.B., and Daley, G.Q. (2012). Reprogramming cellular identity for regenerative medicine. *Cell* **148**, 1110–1122.
- Dhawan, A., Puppi, J., Hughes, R.D., and Mitry, R.R. (2010). Human hepatocyte transplantation: current experience and future challenges. *Nat. Rev. Gastroenterol. Hepatol.* **7**, 288–298.
- Gómez-Lechón, M.J., Donato, M.T., Castell, J.V., and Jover, R. (2004). Human hepatocytes in primary culture: the choice to investigate drug metabolism in man. *Curr. Drug Metab.* **5**, 443–462.
- Graf, T., and Enver, T. (2009). Forcing cells to change lineages. *Nature* **462**, 587–594.
- Guengerich, F.P. (2002). Cytochrome P450 enzymes in the generation of commercial products. *Nat. Rev. Drug Discov.* **1**, 359–366.
- Hanna, J., Saha, K., Pando, B., van Zon, J., Lengner, C.J., Creighton, M.P., van Oudenaarden, A., and Jaenisch, R. (2009). Direct cell reprogramming is a stochastic process amenable to acceleration. *Nature* **462**, 595–601.
- Harvey, M., Sands, A.T., Weiss, R.S., Hegi, M.E., Wiseman, R.W., Pantazis, P., Giovannella, B.C., Tainsky, M.A., Bradley, A., and Donehower, L.A. (1993). In vitro growth characteristics of embryo fibroblasts isolated from p53-deficient mice. *Oncogene* **8**, 2457–2467.
- He, Z., Zhang, H., Zhang, X., Xie, D., Chen, Y., Wangenstein, K.J., Ekker, S.C., Firpo, M., Liu, C., Xiang, D., et al. (2010). Liver xeno-repopulation with human hepatocytes in Fah^{-/-}/Rag2^{-/-} mice after pharmacological immunosuppression. *Am. J. Pathol.* **177**, 1311–1319.
- Hengstler, J.G., Brulport, M., Schormann, W., Bauer, A., Hermes, M., Nussler, A.K., Fandrich, F., Ruhnke, M., Ungefroren, H., Griffin, L., et al. (2005). Generation of human hepatocytes by stem cell technology: definition of the hepatocyte. *Expert Opin. Drug Metab. Toxicol.* **1**, 61–74.
- Huang, P., He, Z., Ji, S., Sun, H., Xiang, D., Liu, C., Hu, Y., Wang, X., and Hui, L. (2011). Induction of functional hepatocyte-like cells from mouse fibroblasts by defined factors. *Nature* **475**, 386–389.
- Ji, S., Zhang, L., and Hui, L. (2013). Cell fate conversion: direct induction of hepatocyte-like cells from fibroblasts. *J. Cell. Biochem.* **114**, 256–265.
- Kiyono, T., Foster, S.A., Koop, J.I., McDougall, J.K., Galloway, D.A., and Klingelutz, A.J. (1998). Both Rb/p16INK4a inactivation and telomerase activity are required to immortalize human epithelial cells. *Nature* **396**, 84–88.
- Kuo, C.J., Conley, P.B., Chen, L., Sladek, F.M., Darnell, J.E., Jr., and Crabtree, G.R. (1992). A transcriptional hierarchy involved in mammalian cell-type specification. *Nature* **355**, 457–461.
- Land, H., Parada, L.F., and Weinberg, R.A. (1983). Tumorigenic conversion of primary embryo fibroblasts requires at least two cooperating oncogenes. *Nature* **304**, 596–602.
- Lázaro, C.A., Chang, M., Tang, W., Campbell, J., Sullivan, D.G., Gretch, D.R., Corey, L., Coombs, R.W., and Fausto, N. (2007). Hepatitis C virus replication in transfected and serum-infected cultured human fetal hepatocytes. *Am. J. Pathol.* **170**, 478–489.
- Li, R., Liang, J., Ni, S., Zhou, T., Qing, X., Li, H., He, W., Chen, J., Li, F., Zhuang, Q., et al. (2010). A mesenchymal-to-epithelial transition initiates and is required for the nuclear reprogramming of mouse fibroblasts. *Cell Stem Cell* **7**, 51–63.
- Liddle, C., and Goodwin, B. (2002). Regulation of hepatic drug metabolism: role of the nuclear receptors PXR and CAR. *Semin. Liver Dis.* **22**, 115–122.
- Liu, X., Chism, J.P., LeCluyse, E.L., Brouwer, K.R., and Brouwer, K.L. (1999). Correlation of biliary excretion in sandwich-cultured rat hepatocytes and in vivo in rats. *Drug Metab. Dispos.* **27**, 637–644.
- Mei, J., Sgroi, A., Mai, G., Baertschiger, R., Gonelle-Gispert, C., Serre-Beinier, V., Morel, P., and Bühler, L.H. (2009). Improved survival of fulminant liver failure by transplantation of microencapsulated cryopreserved porcine hepatocytes in mice. *Cell Transplant.* **18**, 101–110.
- Nam, Y.J., Song, K., Luo, X., Daniel, E., Lambeth, K., West, K., Hill, J.A., DiMaio, J.M., Baker, L.A., Bassel-Duby, R., and Olson, E.N. (2013). Reprogramming of human fibroblasts toward a cardiac fate. *Proc. Natl. Acad. Sci. USA* **110**, 5588–5593.

Figure 7. Rescue of Acute Liver Failure by Encapsulated hiHep^{LT} Cells

- (A) Schematic outline of the use of encapsulated hiHep^{LT} cells for treatment of acute liver failure mice. C57Bl6/J mice were injected with concanavalin A (Con A) to trigger fulminant hepatitis, which led to acute liver failure and death within 12–24 hr in all mice. Eight hours after Con A treatment, 5×10^6 encapsulated PHHs or 1.5×10^7 alginate-poly-L-lysine-alginate (APA)-encapsulated HFFs, HepG2, or hiHep^{LT} cells were injected intraperitoneally into mice with acute liver failure.
- (B) Whereas all mice died upon transplantation of encapsulated HFFs and HepG2 cells, 5 of 15 recipient mice survived after transplantation with encapsulated hiHep^{LT} cells, and 1 of 4 mice receiving PHH cell transplantation survived. The Kaplan-Meier survival curve is depicted.
- (C and D) Serum levels of ALT (C) and AST (D) in Con-A-treated mice before (day 0) and after (day 4 and day 7) transplantation of encapsulated hiHep^{LT} and PHH cells.
- (E and F) Livers (E), macroscopic images of freshly isolated livers) and liver sections (F), hematoxylin and eosin staining) from Con-A-treated mice before (day 0) and after hiHep^{LT} cell transplantation (days 4 and 7). Note Con-A-induced hepatitis and hemorrhage in the liver at day 0 (E) and arrows in (F), residual liver damage at day 4 (E) and arrowheads in (F), and the completely recovered liver at day 7.

* $p < 0.05$, log rank test for (B). See also Figure S7 and Movies S1 and S2.

- Odom, D.T., Dowell, R.D., Jacobsen, E.S., Gordon, W., Danford, T.W., MacIsaac, K.D., Rolfe, P.A., Conboy, C.M., Gifford, D.K., and Fraenkel, E. (2007). Tissue-specific transcriptional regulation has diverged significantly between human and mouse. *Nat. Genet.* **39**, 730–732.
- Orive, G., Hernández, R.M., Rodríguez Gascón, A., Calafiore, R., Chang, T.M., de Vos, P., Hortelano, G., Hunkeler, D., Lacik, I., and Pedraz, J.L. (2004). History, challenges and perspectives of cell microencapsulation. *Trends Biotechnol.* **22**, 87–92.
- Overturf, K., Al-Dhalimy, M., Tanguay, R., Brantly, M., Ou, C.N., Finegold, M., and Grompe, M. (1996). Hepatocytes corrected by gene therapy are selected in vivo in a murine model of hereditary tyrosinaemia type I. *Nat. Genet.* **12**, 266–273.
- Palakkan, A.A., Hay, D.C., Anil Kumar, P.R., Kumary, T.V., and Ross, J.A. (2013). Liver tissue engineering and cell sources: issues and challenges. *Liver Int.* **33**, 666–676.
- Pan, G., Boisselle, C., and Wang, J. (2012). Assessment of biliary clearance in early drug discovery using sandwich-cultured hepatocyte model. *J. Pharm. Sci.* **101**, 1898–1908.
- Pang, Z.P., Yang, N., Vierbuchen, T., Ostermeier, A., Fuentes, D.R., Yang, T.Q., Citri, A., Sebastiano, V., Marro, S., Südhof, T.C., and Wernig, M. (2011). Induction of human neuronal cells by defined transcription factors. *Nature* **476**, 220–223.
- Qiang, L., Fujita, R., Yamashita, T., Angulo, S., Rhinn, H., Rhee, D., Doege, C., Chau, L., Aubry, L., Vanti, W.B., et al. (2011). Directed conversion of Alzheimer's disease patient skin fibroblasts into functional neurons. *Cell* **146**, 359–371.
- Roger, V., Balladur, P., Honiger, J., Baudrimont, M., Delelo, R., Robert, A., Calmus, Y., Capeau, J., and Nordlinger, B. (1998). Internal bioartificial liver with xenogeneic hepatocytes prevents death from acute liver failure: an experimental study. *Ann. Surg.* **228**, 1–7.
- Sekiya, S., and Suzuki, A. (2011). Direct conversion of mouse fibroblasts to hepatocyte-like cells by defined factors. *Nature* **475**, 390–393.
- Shay, J.W., Pereira-Smith, O.M., and Wright, W.E. (1991). A role for both RB and p53 in the regulation of human cellular senescence. *Exp. Cell Res.* **196**, 33–39.
- Sridharan, R., Tchiew, J., Mason, M.J., Yachechko, R., Kuoy, E., Horvath, S., Zhou, Q., and Plath, K. (2009). Role of the murine reprogramming factors in the induction of pluripotency. *Cell* **136**, 364–377.
- Stadtfeld, M., Maherali, N., Breault, D.T., and Hochedlinger, K. (2008). Defining molecular cornerstones during fibroblast to iPS cell reprogramming in mouse. *Cell Stem Cell* **2**, 230–240.
- Tiegs, G., Hentschel, J., and Wendel, A. (1992). A T cell-dependent experimental liver injury in mice inducible by concanavalin A. *J. Clin. Invest.* **90**, 196–203.
- Tiscornia, G., Vivas, E.L., and Izpisua Belmonte, J.C. (2011). Diseases in a dish: modeling human genetic disorders using induced pluripotent cells. *Nat. Med.* **17**, 1570–1576.
- Tsukada, T., Tomooka, Y., Takai, S., Ueda, Y., Nishikawa, S., Yagi, T., Tokunaga, T., Takeda, N., Suda, Y., Abe, S., et al. (1993). Enhanced proliferative potential in culture of cells from p53-deficient mice. *Oncogene* **8**, 3313–3322.
- Vierbuchen, T., and Wernig, M. (2011). Direct lineage conversions: unnatural but useful? *Nat. Biotechnol.* **29**, 892–907.
- Wang, Q., Li, S., Xie, Y., Yu, W., Xiong, Y., Ma, X., and Yuan, Q. (2006). Cytoskeletal reorganization and repolarization of hepatocarcinoma cells in APA microcapsule to mimic native tumor characteristics. *Hepatol. Res.* **35**, 96–103.
- Wong, H., and Chang, T.M. (1986). Bioartificial liver: implanted artificial cells microencapsulated living hepatocytes increases survival of liver failure rats. *Int. J. Artif. Organs* **9**, 335–336.
- Xie, H., Yu, W., Liu, X., Xie, W., Lv, G., Wang, F., and Ma, X. (2011). Basic properties of alginate/chitosan microcapsule surfaces and their interaction with proteins. *J. Control. Release* **152** (Suppl 1), e246–e248.
- Yamanaka, S., and Blau, H.M. (2010). Nuclear reprogramming to a pluripotent state by three approaches. *Nature* **465**, 704–712.
- Yu, Y., Fisher, J.E., Lillegard, J.B., Rodysill, B., Amiot, B., and Nyberg, S.L. (2012). Cell therapies for liver diseases. *Liver Transpl.* **18**, 9–21.
- Zaret, K.S. (2008). Genetic programming of liver and pancreas progenitors: lessons for stem-cell differentiation. *Nat. Rev. Genet.* **9**, 329–340.
- Zaret, K.S., and Grompe, M. (2008). Generation and regeneration of cells of the liver and pancreas. *Science* **322**, 1490–1494.
- Zaret, K.S., and Carroll, J.S. (2011). Pioneer transcription factors: establishing competence for gene expression. *Genes Dev.* **25**, 2227–2241.